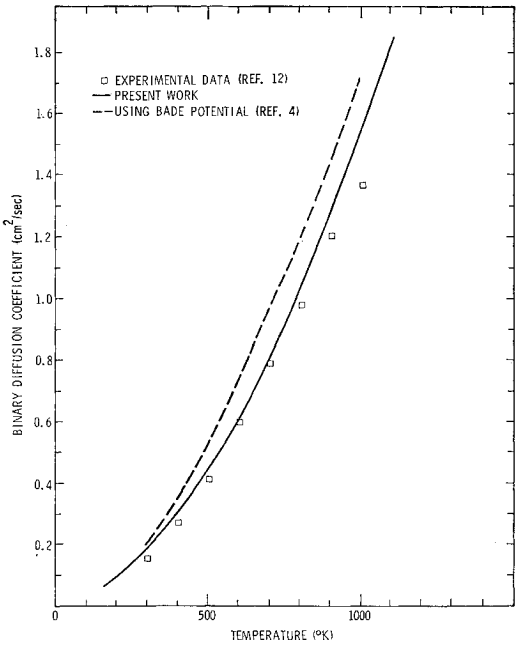

Fig. 3 Comparison of theoretical and experimental binary diffusion coefficients for carbon dioxide and molecular oxygen (at one atmosphere).

for viscosity from which $T_1(r_{ms})$ was determined. It shows the value of $T_1^{1/3}$ required in Eqs. (2–4) to be $10/Y$. A similar plot for diffusion demonstrated the same dependence on r_{ms} as for viscosity except that Y(for diffusion) = $0.6Y$(viscosity).

Figures 2 and 3 contain the values of the transport coefficients obtained using the method described in this Note. Figures 2 and 3 also contain results obtained using other theoretical calculations by Bade[4] and Devoto.[11] Both of these calculations use a somewhat more complicated potential (exponential repulsive) and handle gas mixtures in a different manner. The relative decrease in the viscosity of argon for temperatures above 9000°K obtained by Devoto is due to the effects of ionization which are not included in the calculations contained in this Note. As is shown in the figures, coefficients obtained from the method given in this Note are close enough to experimental results to be useful in most flowfield calculations.

References

[1] Moore, J. A., "Approximate Transport Coefficients for Neutral-Neutral Interactions," Rept. MDAC-WD1117, Sept. 1969, McDonnell Douglas Astronautics Co., Huntington Beach, Calif.

[2] Hirschfelder, J. O., Curtiss, C. F., and Bird, R. B., *Molecular Theory of Gases and Liquids*, Wiley, New York, 1954, a) p. 960, b) p. 952, and c) p. 963.

[3] Hirschfelder, J. O. and Eliason, M. O., "The Estimation of the Transport Properties for Electronically Excited Atoms and Molecules," Tech. Rept. WIS-AF-1, May 1956, Univ. of Wisconsin, Milwaukee, Wis.

[4] Bade, W. L., "Empirical Interatomic and Intermolecular Potentials," 2-TM-58-42, April 1958, AVCO Research and Advanced Development Laboratory, Wilmington, Mass.

[5] Carnvale, E. H. et al., "Experimental Determination of Transport Properties of High Temperature Gases," Contractor Report CR-789, June 1967, NASA, Washington, D. C.

[6] Kanzawa, A. and Kimara, I., "Measurements of Viscosity and Thermal Conductivity of Partially Ionized Argon Plasmas," *AIAA Journal*, Vol. 5, No. 7, July 1967, pp. 1315–1319.

[7] Soo, S. L. and Bahadari, M. N., "Boundary Layer Motion in a Two-Dimensional Arc-Heated Channel," AGARDograph 84, Part II, Sept. 1964, Advisory Group for Aerospace Research and Development, North Atlantic Treaty Organization, p. 1013.

[8] Bonilla, C F., Wang, S. J., and Weiner, H., "The Viscosity of Steam, Heavy Water Vapor, and Argon at Atmospheric Pressure Up to High Temperatures," *Transactions of the ASME*, Vol. 78, 1956, pp. 1285–1289.

[9] Collins, D. J. and Menard, W. A., "Measurement of the Thermal Conductivity of Noble Gases in the Temperature Range 1500 to 5000 Deg Kelvin," *Transactions of the ASME, Ser. C*, Vol. 88, 1966, pp. 52–56.

[10] Aeschliman, D. P., Ph.D. thesis, 1968, Northwestern University, Evanston, Ill.

[11] Devoto, R. S., "Transport Coefficients of Partially Ionized Argon," *The Physics of Fluids*, Vol. 10, No. 2, Feb. 1967, pp. 354–371.

[12] Fristrom, R. M. and Westenberg, A. A., *Flame Structure*, McGraw-Hill, New York, 1965, p. 265.

Spectrum of MPD Arc Oscillations at Low-Magnetic Field

D. J. CONNOLLY*
NASA Lewis Research Center, Cleveland, Ohio

Introduction

IN MPD thruster operation, one has a critical magnetic field below which the discharge is quiet and axisymmetric.[1–3] Above this field the discharge is concentrated into a rotating current spoke. The plasma rotates whether the spoke is present or not.[3] One would expect some sort of transition region where the discharge varies in a continuous way from the spoke to the no-spoke mode. Previous experiments[2] indicate that there is no such region.

Measurements with segmented anodes[3,5] indicate that the current spoke is a highly nonlinear phenomenon. Most of the current is concentrated in the rotating spoke. In analysis, however, it is often necessary to treat the disturbances as small perturbations.[6,7] It seemed desirable, therefore, to look for a region where the disturbances really were small. Further investigation at magnetic fields just below threshold seemed appropriate.

Apparatus

The thruster used (Fig. 1) is a McDonnell-Douglas X-7 and is described in Ref. 4. The discharge was probed with a

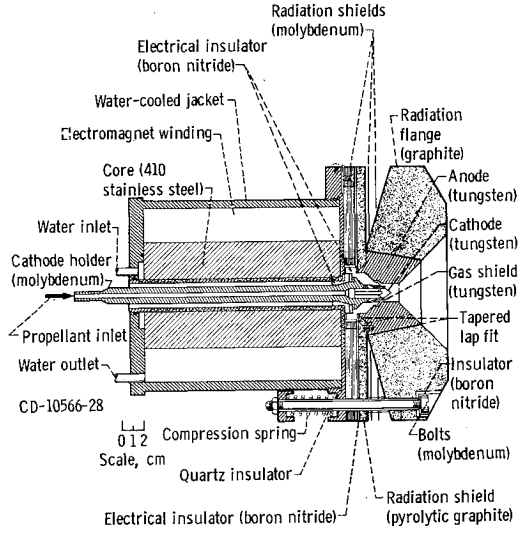

Fig. 1 Schematic drawing of McDonnell-Douglas X-7 thruster.

Received June 12, 1970.
*Aerospace Research Engineer.

0.030-in. diameter plane probe. The probe is brought in through a hole in the anode as shown in Fig. 2. It is arranged to be flush with the anode surface in the region of maximum current attachment. The hole in the anode is 0.058 in. in diameter at the inner face of the anode. The probe is retained in the center of the hole by magnesium oxide tubing which fills the remainder of the hole. The current collected by the probe is returned to anode potential through a 1.1Ω resistor. The voltage developed across the resistor is carried to the control room by a pair of identical coaxial cables terminated in their characteristic impedance (50Ω). The signal is then carried through a differential amplifier to a spectrum analyzer.

Preliminary Results

A typical sequence of arc current spectra is shown in Fig. 3. Figure 3a is obtained just below the threshold magnetic field; Fig. 3b just above it and Fig. 3c at normal operating field. In each spectrum the horizontal scale is from 0 to 2.5 Mhz. The large spike at zero frequency is due to the local oscillator component in the output of the mixer and is always present.

The spectra of Fig. 3 are typical of the cases studied. Below the threshold magnetic field there is a small but well defined spectrum of oscillations in the probe current. The spectrum is concentrated in a series of peaks with spacing of order 400 khz. The amplitude of the peaks decreases gradually with frequency. The signal typically has significant components out to about 10 Mhz.

The spectrum of small oscillations is present from threshold magnetic field ($0.05T$) down, at least to the lowest magnetic field studied—about $0.025T$.

Increasing the magnetic field to slightly above the threshold value causes a sudden transition to the rotating spoke regime (Fig. 3b). There is a two-order of magnitude increase in the amplitude of the oscillations and a sharp increase in the arc voltage as well. The spectrum is furthermore dominated by a large peak around 300 khz, the rotating spoke frequency. As the magnetic field is further increased, there is a gradual increase in arc voltage and amplitude of the oscillations. Also the single peak at the rotating spoke frequency becomes progressively more dominant.

The rotating spoke frequency did not change appreciably with magnetic field, arc current, or mass flow rate when this thruster was operated on ammonia propellant. When operating on hydrogen propellant, the frequency had the expected dependence on these parameters. It increased with increasing arc current and magnetic field strength and decreased with increasing mass flow rate.

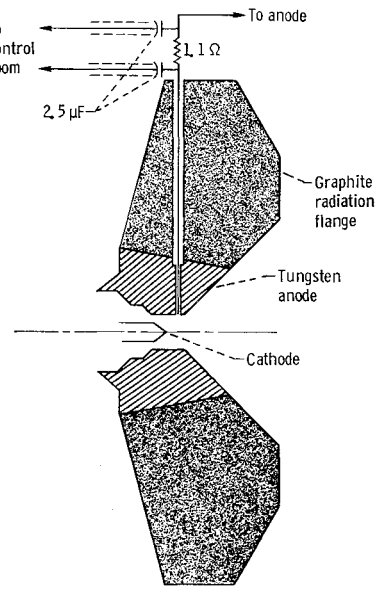

Fig. 2 Diagnostic probe arrangement.

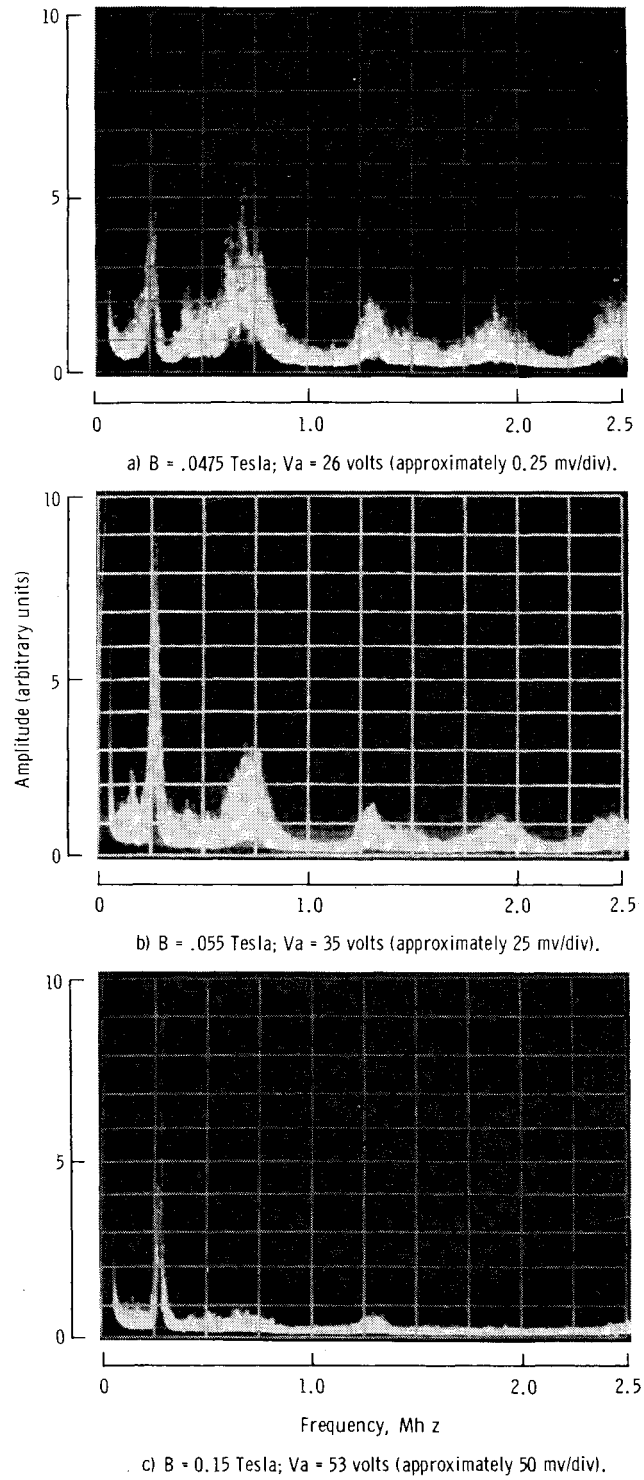

Fig. 3 Arc current spectra (0 to 2.5 mc); total arc current = 400 amps; ammonia flow rate = 0.04 g/sec.

Concluding Remarks

At least in some cases the MPD thruster has a spectrum of small oscillations at low-axial magnetic field. As the magnetic field is increased above the threshold value, the oscillations evolve into a rotating current spoke. The latter is a highly nonlinear phenomenon, and linearized or even quasi-linear theories are questionable in this regime. Such theories would not be subject to the same objection in the region around and below the threshold magnetic field. Here the oscillations are smaller. Ability to predict the spectrum of oscillations in this regime would be a useful test of such theories. And the experimental connection between the

small oscillation region and the spoke region may show how to extend quasi-linear calculations to apply in the latter.

References

[1] Malliaris, A. C., "Investigation of Acceleration Mechanisms in MPD Accelerators," ARL 68-0078, April 1968, U. S. Air Force Aerospace Research Lab., Wright-Patterson Air Force Base, Ohio.

[2] Allario, F., Jarrett, O., Jr., and Hess, R. V., "Onset of Rotating Disturbances in the Interelectrode Region and Exhaust Jet of an MPD Arc," AIAA Paper 69-232, New York, 1969.

[3] Larson, A. V., "Experiments on Magnetoplasmadynamic Engines with Rotating Current Distributions," NASA CR-66803, June 1969, General Dynamics/Convair, San Diego, Calif.

[4] Esker, D. W., Kroutil, J. C., and Checkley, R. J., "Radiation Cooled MPD Arc Thruster," MDC-H296, NASA-CR-72557, July 1969, McDonnell-Douglas Co., St. Louis, Mo.

[5] Larson, A. V., "Experiments on Current Rotations in an MPD Engine," *AIAA Journal*, Vol. 6, No. 6, June 1968, pp. 1001–1006.

[6] Smith, J. M., "Electrothermal Instability—An Explanation of the MPD Arc Thruster Rotating Spoke Phenomenon," AIAA Paper 69-231, New York, 1969.

[7] Hassan, H. A. and Thompson, C. C., "Onset of Instabilities in Coaxial Hall Current Accelerators," *AIAA Journal*, Vol. 7, No. 12, Dec. 1969, pp. 2300–2304.

Note on an Approximate Method for Computing Nonconservative Generalized Forces on Finitely Deformed Finite Elements

J. T. ODEN*

Research Institute, The University of Alabama, Huntsville, Ala.

Introduction

In the analysis of finite deformations of deformable bodies by the finite-element method, surface tractions acting on material surfaces in the deformed body are replaced by consistent generalized forces which are concentrated at nodal points on the element boundaries. Typically, the character of these generalized forces is determined on the basis of invariance of the potential energy of the external forces and independence of path of the deformation process, a procedure which tacitly assumes that the forces are conservative. In practical applications, however, the applied forces are rarely conservative. Even in the case of relatively simple loadings (e.g., uniform external pressures), the net generalized forces are not conservative, and in order to account for their variation in magnitude as the body deforms they must be expressed as functions of the displacement gradients at the element boundaries.[1–3] Unfortunately, when correct expressions for consistent nonconservative generalized forces on finitely deformed elements are obtained, they often appear as extremely complicated functions of the nodal displacements. This complexity possibly explains why such forces have rarely been used in finite-element analyses of geometrically nonlinear problems.

In this Note, a relatively simple approximate technique is discussed which leads to simple formulas for nonconservative generalized nodal forces on finitely deformed finite elements. Special cases appropriate for normal pressures are also cited.

Received February 2, 1970; revision received by August 3, 1970. The support of this work by the U. S. Air Force Office of Scientific Research under Contract F44620-69-C-0124 is gratefully acknowledged.

* Professor of Engineering Mechanics. Member AIAA.

Nonconservative Generalized Forces

Consider a discrete model of an arbitrary continuous body which consists of a collection of finite elements connected together at various nodal points. When the body is in a reference configuration C_0, we establish a system of material coordinates x^i, $i = 1$–3, which, for simplicity, are assumed to be rectangular Cartesian, and a corresponding system of orthonormal base vectors i_i. A typical finite element e with N_e nodal points is isolated from the collection, the volume, surface area, and mass density of which are denoted $v_{0(e)}$, $A_{0(e)}$, and ρ_0 while in C_0. Following the usual finite-element procedure, the local displacement field $u_i(\mathbf{x},t)$ over e at time t is approximated by

$$u_i(\bar{x},t) = \psi_N(\mathbf{x})u_i{}^N \tag{1}$$

where N is summed from 1 to N_e, $\psi_N(\mathbf{x})$ are local interpolation functions, and $u_i{}^N = u_i{}^N(t)$ are the components of displacement at node N of the element. With the aid of Eq. (1), all other kinematical quantities can be determined. It is not difficult to show that the components of generalized force at node N are

$$p_{Ni} = \int_{v_{0(e)}} \rho_0 \hat{F}_i \psi_N dv_0 + \int_{A_{0(e)}} \hat{S}_0{}^j(\delta_{ji} + \psi_{M,j}u_i{}^M)\psi_N dA_0 \tag{2}$$

where $\hat{F}_i$ are components of body force and $\hat{S}_0{}^j$ are components of surface tractions referred to the convected coordinate lines x^i in the deformed body.

The contribution of body forces to p_{Ni} of Eq. (2) present no special problems since the components $\hat{F}_i(\mathbf{x},t)$ are assumed to be prescribed for all $\mathbf{x}$ and t. The surface integral, however, is generally a complicated function of $u_i{}^N$. For example, in the case in which the material surface of a finite element is subjected to a normal traction $q = q(\mathbf{x},t)$,

$$\hat{S}^j = qG^{1/2}G^{jk}\hat{n}_k \tag{3}$$

where G^{jk} is the inverse of $G_{ij} = (\delta_{im} + \psi_{M,i}u_m{}^M)(\delta_{jm} + \psi_{N,j}u_m{}^N)$, $G = \det G_{ij}$, and $\hat{n}_k$ are the components of a unit vector normal to the undeformed area A_0.

Approximate Forms

Since the generalized nodal forces are quite complicated functions of the nodal displacements, it is natural to seek simplified approximations of these forces. We shall describe one rather general method of approximation which amounts to representing the deformed surface area of an arbitrary finite element by a collection of flat triangular or quadrilateral elements over which the loading is assumed to be uniform.

Consider the surface of an arbitrary type of finite element, as shown in Fig. 1, which undergoes large displacements and distortions due to a general system of applied surface tractions. We ignore body forces here since they are adequately accounted for by Eq. (2). Regardless of the actual form of the local displacement field $u_i = \psi_N u_i{}^N$, we represent the deformed material surface by a collection of flat elements, generally triangular in shape, the nodal points of which are coincident with those of the original material surface of the element. The applied surface tractions per unit surface area are assumed to be uniform over each flat element. Ideally, if the element is sufficiently small the network of subelements can provide a close approximation to rather general applied loads.

Confining our attention to a typical flat triangular subelement of area a, let $\bar{n}$, $\bar{e}_1$, and $\bar{e}_2$ denote an orthonormal triad of